

Bifurcations on Potential Energy Surfaces of Organic Reactions

Daniel H. Ess, Steven E. Wheeler, Robert G. Iafe, Lai Xu, Nihan Çelebi-Ölçüm, and Kendall N. Houk*

bifurcations · bis-pericyclic transition states ·
reaction mechanisms ·
theoretical chemistry calculations ·
valley-ridge inflection point

A single transition state may lead to multiple intermediates or products if there is a post-transition-state reaction pathway bifurcation. These bifurcations arise when there are sequential transition states with no intervening energy minimum. For such systems, the shape of the potential energy surface and dynamic effects, rather than transition-state energetics, control selectivity. This Minireview covers recent investigations of organic reactions exhibiting reaction pathway bifurcations. Such phenomena are surprisingly general and affect experimental observables such as kinetic isotope effects and product distributions.

1. Introduction

A transition state (TS) is the highest energy point along the minimum-energy path connecting reactants and products, usually connecting one set of reactants with one set of products. However, a single transition state can be shared by two or more reaction pathways if there is a post-transition-state bifurcation. Bifurcations occur when there are sequential transition states with no intervening energy minimum; such a surface involves a valley-ridge inflection (VRI),^[1] where the potential energy surface (PES) valley changes into a dynamically unstable ridge (Figure 1).^[2] This type of potential energy surface describes a reaction mechanism that is different from stepwise or concerted and has been referred to as a two-step-no-intermediate mechanism.^[3] When a reaction has this type of surface, the rate of selective formation of one product relative to another is governed by the potential energy surface shape and resulting dynamic effects.^[4]

Early reported examples of bifurcating reactions involved simple isomerizations, rearrangements, and addition reactions. These include, for example, bond shifting of cyclooctatetraene, ring opening of cyclopropylidene, and the addition of HF to ethylene.^[2,5] Recently, however, several complex organic reactions, most notably pericyclic reactions, have been shown to involve bifurcating reaction pathways. This Minireview covers recent examples of isomerizations, substitutions, and pericyclic reactions that involve reaction pathway bifurcations.

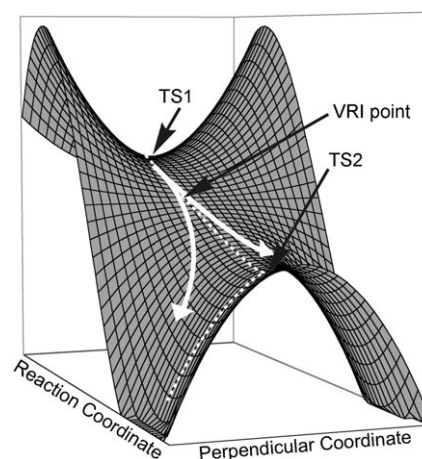


Figure 1. Model potential energy surface with sequential transition states. Dotted white lines represent the IRC pathway while solid lines represent expected reaction trajectories.

[*] Dr. D. H. Ess, Dr. S. E. Wheeler, R. G. Iafe, L. Xu, N. Çelebi-Ölçüm, Prof. K. N. Houk
Department of Chemistry and Biochemistry
University of California, Los Angeles
607 Charles E. Young Drive East, Los Angeles, CA 90095 (USA)
Fax: (+1) 310-206-1843
E-mail: houk@chem.ucla.edu

A stationary point on a molecular PES is a point in the $3N-6$ dimensional configuration space in which the energy gradients (forces) with respect to nuclear positions are all zero.^[6] Characterization of a stationary point as either a minimum or saddle point requires the evaluation of second derivatives, or force constants. When all second derivatives are positive, the stationary point is a minimum, while one negative second derivative indicates a saddle point.^[7] In typical quantum mechanical calculations, characterization of stationary points is achieved by diagonalizing the matrix of mass-weighted second derivatives (the Hessian matrix) to yield normal vibrational modes (eigenvectors) and the associated force constants (eigenvalues).^[6]

Along the floor of a downward sloping valley, one gradient is negative and all others are zero, with positive force constants. If two transition states occur sequentially with no intervening energy minimum, the curvature of the energy surface along one direction perpendicular to the reaction coordinate must change from positive to negative; that is, the valley floor becomes a ridge at some point in this two-dimensional configuration space. The point where this occurs is the valley-ridge inflection point. Here the Hessian has one zero eigenvalue corresponding to a motion perpendicular to the gradient.^[7] Near the VRI, the single reaction pathway

branches into two; there is no longer a restoring force for molecular motion perpendicular to the reaction coordinate. However, unlike minima and saddle points, the location of a VRI point is dependent upon the choice of coordinate systems.^[8]

The intrinsic reaction coordinate (IRC) is the most common quantum mechanical reaction pathway description (Figure 1).^[9] This is a mass-weighted steepest descent path, following the negative gradient downhill from a transition state. Physically, the IRC corresponds to the pathway travelled by nuclei moving on the PES with infinitesimal velocities and is typically considered the theoretical minimum-energy pathway (MEP). However, when the gradient becomes zero or a potential energy surface is flat, a single IRC cannot describe a unique preferred reaction trajectory.^[10]

Figure 1 shows the difference between an IRC pathway (dotted lines) and qualitative dynamics trajectories (white arrows) for a symmetrical model PES with two sequential transition states (TS1 and TS2) and an intervening VRI point. The IRC is the steepest descent pathway from TS1 and follows the valley floor in this region. After passing through the VRI point, the IRC stays on the developing ridge before stopping at TS2. From TS2, the IRC exhibits the typical reaction pathway behavior, following the normal coordinate



Daniel H. Ess completed his undergraduate studies at Brigham Young University and then spent two years as a full-time volunteer for the Church of Jesus Christ of Latter-day Saints. He completed his Ph.D. under the direction of K. N. Houk and is currently a post-doctoral scholar at California Institute of Technology with William A. Goddard III and at The Scripps Research Institute in Florida with Roy A. Periana.

Steven E. Wheeler was born in Richmond, Virginia. He graduated from New College of Florida with a B.A. in Chemistry and Physics. He completed his Ph.D. in Fritz Schaefer's group at the University of Georgia before joining the Houk group as a postdoc in 2006. He is currently an NIH NRSA postdoctoral fellow, studying the prediction of catalytic proficiencies of enzymes, enzyme design, and π -stacking interactions.

Robert G. Iafe was born in San Diego, California in 1982. He graduated with Honors in 2004 from Loyola Marymount University with a B.S. in Chemistry. He completed his M.S. in Ken Houk's group at UCLA. He is currently pursuing his Ph.D. in chemistry, studying pericyclic reaction mechanisms and C-H activation using transition metals under the supervision of Ken Houk and palladium-mediated coupling reactions with Craig Merlic.

Lai Xu was born in Lanzhou, China in 1983. She graduated in 2005 from Peking University in China with a B.S. in chemistry. She is currently a graduate student in the Houk group at UCLA, studying dynamics of 1,3-dipolar cycloaddition reactions.

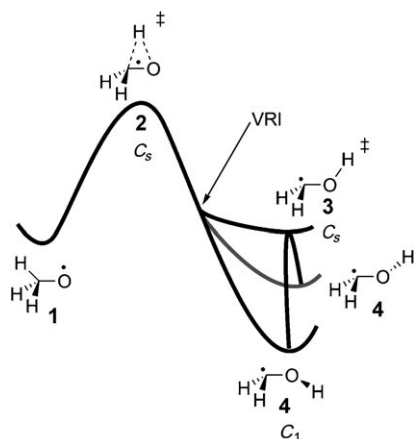
Nihan Çelebi-Ölçüm received her B.S. degree from Boğaziçi University (Istanbul, Turkey) in 1997 and her M.S. degree in Computational and Theoretical Chemistry from Université Henri Poincaré (Nancy, France) in 1999. She then worked for Nevzat Pharmaceuticals, Analytical R&D Department (Istanbul) until 2004. She is currently a Ph.D. student under the direction of Prof. V. Aiyente at Boğaziçi University and has been a visiting graduate student at UCLA.

K. N. Houk was an undergraduate and graduate student at Harvard, working with R. B. Woodward. He has been on the faculties of LSU, the University of Pittsburgh, and UCLA. He received the American Chemical Society James Flack Norris Award in Physical Organic Chemistry and the Award for Computers in Chemical and Pharmaceutical Research. His group is involved with the exploration of organic and biological reactions with computational methods.

corresponding to the imaginary vibrational frequency, connecting the two products. Representative reaction trajectories that would result from dynamics simulations are depicted by the white arrows and show that typical trajectories deviate from the IRC in the vicinity of the VRI, bypassing TS2.^[11] Several groups are actively investigating alternative theoretical treatments of hypersurfaces to rigorously define a reaction pathway when a VRI occurs.^[12] Methods include reaction-path Hamiltonians,^[13] reduced gradient following,^[14] gradient extremals,^[15] transition path sampling,^[16] and the distinguished coordinate method.^[17]

2. Unimolecular Isomerization Reactions

One of the most thoroughly studied reactions with a reaction pathway bifurcation is the isomerization of methoxy radical (**1**, Scheme 1). Ab initio, DFT, and dynamics simu-



Scheme 1. Isomerization of methoxy radical to hydroxymethylene radical.

lation studies all yield similar conclusions about the PES shape and mechanism of this rearrangement.^[12,18–20] Scheme 1 shows the potential energy hypersurface in terms of the COH angle and one of the HCOH dihedral angles. The reaction first proceeds through a three-membered C_s transition state for hydrogen migration (**2**). The reaction pathway bifurcates between TS **2** and TS **3** owing to an intervening VRI. After the VRI, the OH group rotates in or out of the COH plane, leading to either of the equivalent forms of **4**. TS **3**, corresponding to rotation about the C–O bond, arises from the OH bond eclipsing the half-filled hybridized methylene orbital.

Studies on the monodeuterated methoxy radical derivative, H_2DCO ,^[18] have provided insight into vibrational effects on the product ratio. In the all-hydrogen case, the mass-weighted PES is symmetrical, leading to equal reaction-pathway branching toward two equivalent forms of **4**. However, for the deuterium-substituted version, ab initio wave packet dynamics simulations have shown that the slight asymmetry induced by a deuterium atom creates a branching preference in which the hydrogen atom is transferred *cis* to

the deuterium atom on the now slightly unsymmetrical mass-weighted PES.^[19]

The complete active space self-consistent field (CASSCF) PES for cyclooctatetraene (COT) bond shifting is shown in Figure 2.^[21–23] Starting from one of the D_{2d} -symmetric tub

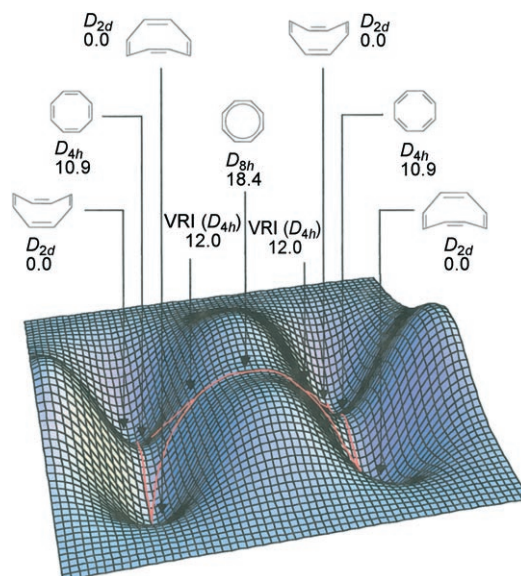


Figure 2. CASSCF/6-31G* potential energy surface for the bond shifting of cyclooctatetraene. Reprinted from reference [23].

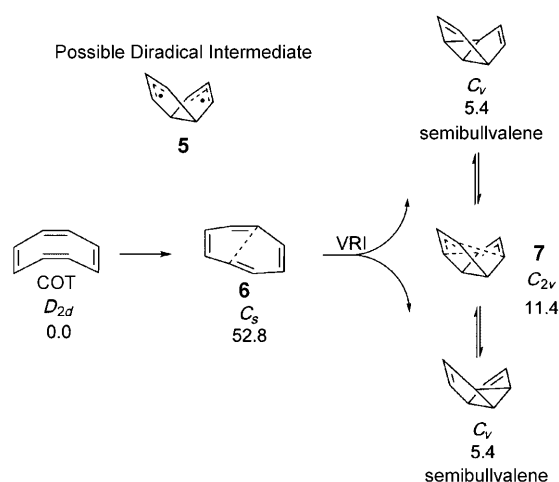
structures, there is a flat D_{4h} saddle point corresponding to tub inversion with localized alternating single and double bonds. This saddle point can be converted to an equivalent D_{4h} -symmetric structure by passing through the planar, antiaromatic D_{8h} saddle point. Alternatively, starting from this D_{8h} -symmetric saddle point, there are two bifurcating reaction pathways leading directly to four equivalent tub structures, bypassing the D_{4h} structures (red lines). Features of this complex PES have been confirmed by a photodetachment study of the COT anion.^[22]

There is also a bifurcation along the reaction pathway for the transformation of COT to semibullvalene (Scheme 2).^[24] Instead of involving the bicyclo[3.3.0]octadiendiyl diradical **5** in a stepwise process, the CAS(MP2)/CASSCF PES computed by Castaño and co-workers suggests that this reaction first proceeds through the rate-determining TS **6**. The reaction pathway then branches between **6** and the Cope TS **7**, yielding either of the equivalent forms of semibullvalene.

Other isomerization reaction pathways with bifurcations include the transformation of fulminic acid (HCNO) to isocyanic acid (HNCO),^[25] ketene–ketenimine rearrangement,^[26] and the photochemical formation of singlet carbene and N_2 from diazirine, in which the bifurcation leads to two different S_0/S_1 conical intersections.^[27]

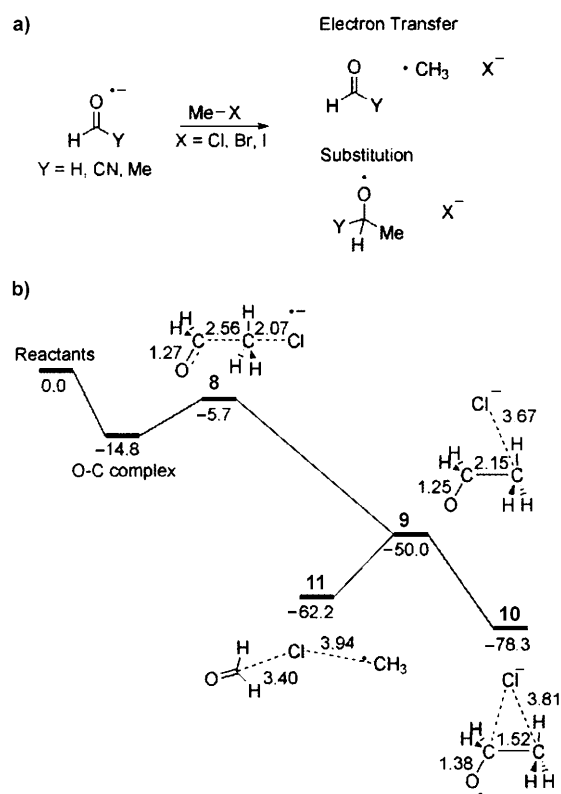
3. Substitution Reactions

Addition of aldehyde radical anion to alkyl halides is hypothesized to occur either by electron-transfer (ET) or



Scheme 2. Stationary points along the CAS(MP2)/CASSCF PES for the transformation of COT to semibullvalene. Energy values (in kcal mol⁻¹) taken from reference [24].

substitution mechanisms (Scheme 3 a). Shaik and co-workers have shown that these mechanisms actually involve a common transition state and a PES bifurcation.^[28] Scheme 3 b outlines the computed ab initio PES for the reaction of formaldehyde radical anion with methylchloride. After an



Scheme 3. a) Substitution and electron-transfer reactions for aldehyde radical anion additions to alkyl halides. b) (U)QCISD(T) PES for the reaction of formaldehyde radical anion with methylchloride. IRC starting at **8** leads to **10**, while the reaction path in non-mass-weighted coordinates leads from **8** to **11**. Energies and configurations taken from reference [28].

initial van der Waals complex, there is an electron-transfer TS (**8**) immediately followed by the TS for radical addition (**9**). Because of a PES bifurcation, the mass-weighted IRC leads from **8** to the C-substitution product **10** (which was not the experimentally observed major product), whereas the steepest descent path in non-mass-weighted coordinates connects TS **8** to the electron-transfer product **11**.

Schlegel, Shaik, and co-workers^[29] and others^[30] provided further insight into this system on the basis of ab initio molecular dynamics simulations of formaldehyde and NCCO radical anions with methyl chloride and fluoride. The predicted product distribution for the reaction in Scheme 3 b at 298 K was 54:12:12:22 for ET, C-substitution, O-substitution, and return to reactants, respectively. The branching ratio was roughly correlated with the C–C bond length in the electron-transfer transition state; long C–C bonds in **8** lead to **11**, while short C–C bonds lead to **10**.

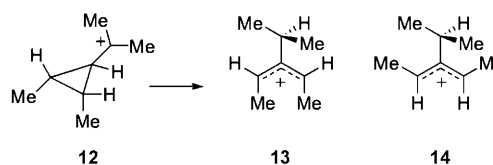
4. Pericyclic Reactions

4.1. Electrocyclic reactions

One of the earliest identified examples of a PES bifurcation was reported by Valtazanos et al. for the ring opening of cyclopropylidene (**R**) to allene (**P₁/P₂**, Figure 3 a).^[2,31] Their computed MCSCF hypersurface, mapped with the coordinates for the average conrotatory angle (δ) and the ring-opening C–C–C bond angle (ϕ), is shown in Figure 3 b. In cyclopropylidene, the methylene groups are orthogonal to the ring plane ($\delta = 90^\circ$, $\phi = 55^\circ$). In the initial stages of the reaction, δ remains constant at 90° , and only disrotatory motion (change in ϕ) occurs. The first of two sequential transition states involves a C–C–C ring angle increase to 80° in combination with disrotatory movement of the methylene groups while maintaining C_s symmetry until the C–C bond is broken. As the ring angle increases further, the steepest descent path leads to the transition state that interconverts equivalent allene structures by methylene group rotation. The reaction pathway bifurcates near the VRI point (located at $\delta \approx 90^\circ$ and $\phi \approx 84^\circ$), thus allowing conrotatory displacement to mix into the reaction pathway, breaking C_s symmetry.

Using B3LYP-DFT, Nouri and Tantillo found that the sigmatropic shift and electrocyclic ring opening steps for cyclopropylcarbinyl carbocation **12** occur sequentially with no intermediate.^[32] On this PES, the shared TS is for the 1,2-hydride shift, followed by the disrotatory ring-opening TS. The reaction pathway bifurcates, leading to allyl cation **13** or **14**.

Birney and co-workers have reported an electrocyclic ring opening with an uphill PES bifurcation for the thermal



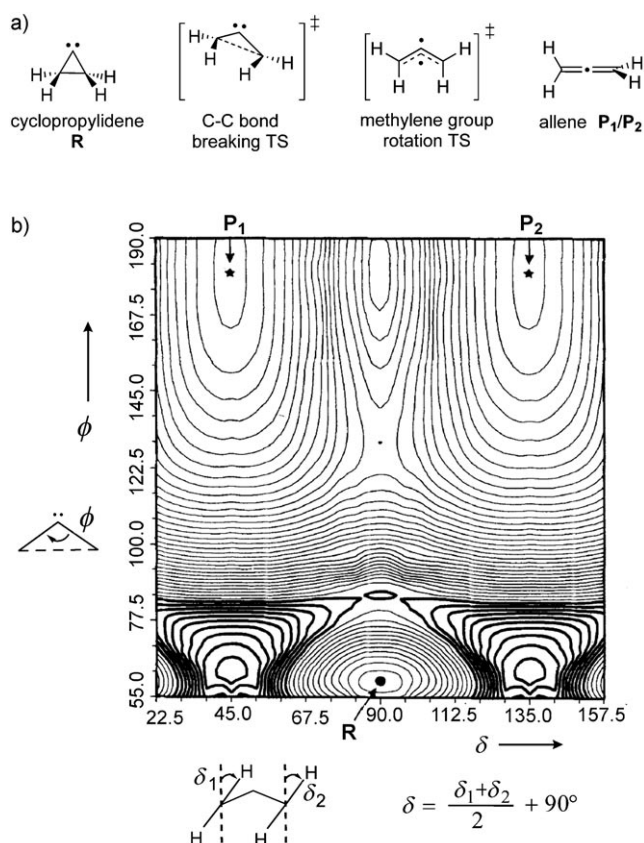
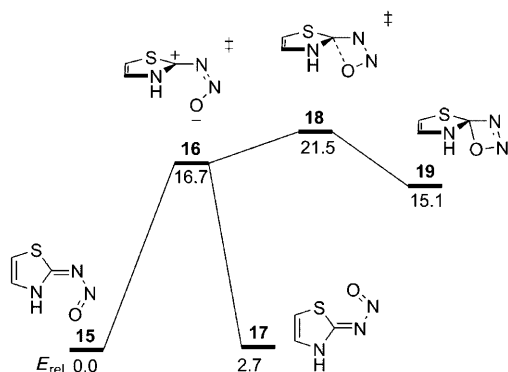


Figure 3. a) Cyclopropylidene (R) to allene (P₁/P₂) rearrangement stationary points. b) MCSCF potential energy surface. Reprinted with permission from reference [2]. Copyright Springer 1986.

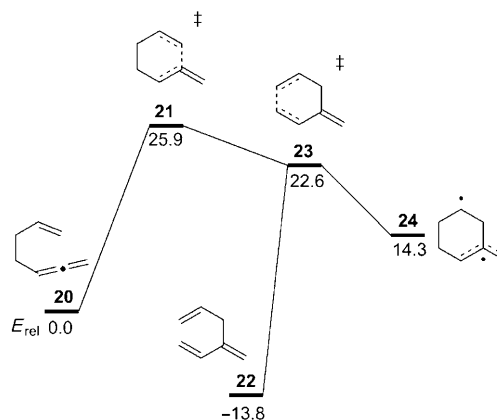
deazetization reaction of heterocyclic nitrosimine **15** (Scheme 4).^[33] The reaction proceeds by sequential transition states for C–N bond rotation (**16**) and pseudopericyclic cyclization (**18**), which then leads to N₂ loss via intermediate **19**. Interestingly, the analogous ring opening of oxetene gives only one concerted transition state, mixing ring opening and dihedral rotation motions simultaneously.



Scheme 4. MP4SDQ stationary points for the thermal deazetization of heterocyclic nitrosimines. Energies taken from reference [33] (in kcal mol^{−1}).

4.2 Sigmatropic Rearrangements

Hrovat, Duncan, and Borden have investigated the Cope rearrangement of 1,2,6-heptatriene **20** (Scheme 5).^[34] Evi-



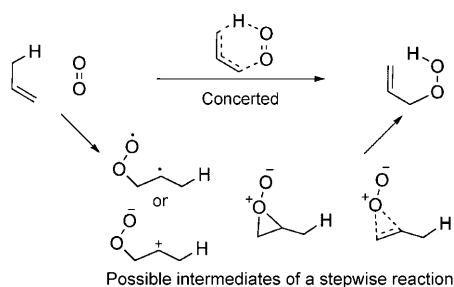
Scheme 5. PES for the rearrangement of 1,2,6-heptatriene (**20**) to 3-methylene-1,5-hexadiene (**22**). IRC calculations using DFT lead from **21** to **22**, while the IRC computed using CASSCF connects **21** to **24**. CASPT2(8,8)/6-31G* energies (kcal mol^{−1}) taken from reference [34].

dence of both stepwise and concerted mechanisms has been observed experimentally.^[35] However, Borden and co-workers only found a single concerted TS (**21**). Formation of either the concerted rearrangement product (**22**) or the diradical intermediate (**24**) was predicted, depending on whether an IRC was computed using DFT or CASSCF methods. Dynamics simulations using a reparameterized semiempirical molecular orbital (MO) model (AM1-SRP) fit to CASSCF stationary points showed that 17 % of the trajectories follow a “concerted” pathway.^[36] Houk and co-workers have identified a similar type of bifurcation on the PES for the rearrangement of 6-methylenebicyclo[3.2.0]hept-2-ene, which yields a diradical intermediate or 5-methylenenorbornene.^[37]

Bifurcations also exist on the PESs for the rearrangements of *cis*-bicyclo[6.1.0]nona-2,4,6-triene, 9,9-dicyanobicyclo[6.1.0]nona-2,4,6-triene,^[38] *cis*-1,2-divinylcyclobutane, and *cis*-1,2-divinylcyclopropane.^[39] In these reactions, the *C_s*-symmetric Cope transition state is followed by the *C_s* boat interconversion transition state with no intervening intermediate. In each case, the result is a bifurcating reaction pathway that leads to either of two equivalent boat structures.

4.3 Ene Reactions

The mechanism of the singlet-oxygen ene reaction has been studied extensively.^[40] Three mechanisms—concerted, stepwise, and exciplex perepoxide formation—have all been proposed on the basis of experimental and theoretical considerations (Scheme 6). Early ab initio studies favored a stepwise mechanism,^[41] while measured kinetic isotope effects (KIEs) and observed stereospecific suprafacial product



Scheme 6. Concerted and stepwise mechanisms for the singlet-oxygen ene reaction.

formation suggest a concerted mechanism or perepoxide mechanism.^[42]

A collaborative effort by the Singleton, Houk, and Foote groups used ¹³C KIEs and quantum mechanical methods to show that this reaction takes place through a two-step-no-intermediate mechanism.^[3,43] CCSD(T) single-point energies computed on a grid of B3LYP structures revealed that the PES bifurcates after a common TS (**26**; Figure 4). The second sequential TS **27** is the elusive perepoxide-like structure with shorter partial C–O bond lengths and connects the two ene products. When branching occurs on this surface, the C–H

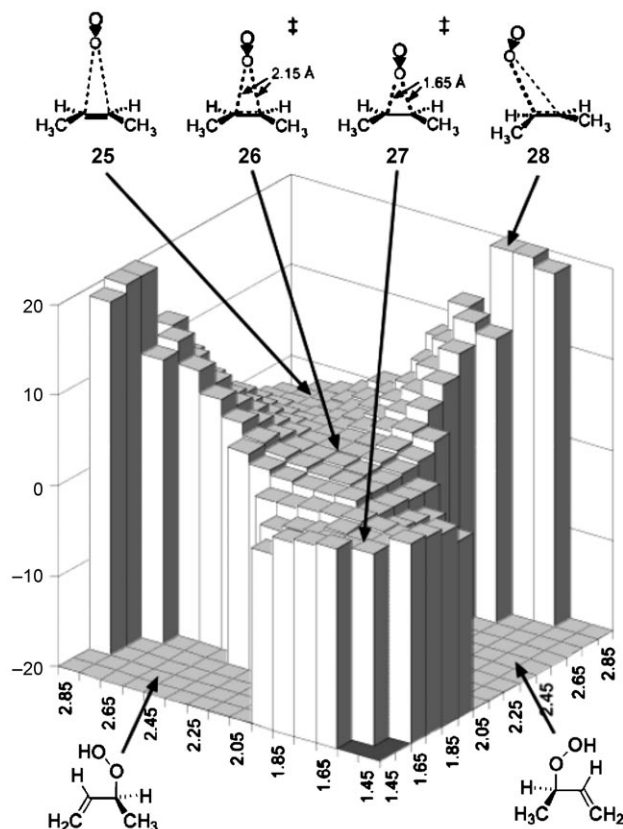


Figure 4. CCSD(T)//B3LYP potential energy surface of the singlet-oxygen ene reaction mapped according to the average alkene C–O separations. Adapted with permission from reference [3]. Copyright 2003 American Chemical Society.

bond breaks and an O–H bond forms. Quasiclassical dynamics simulations on a B3LYP surface^[44] predicted $k_H/k_D = 1.38$, close to the experimental value of approximately 1.4. The origin of this isotope effect is different from that of typical isotope effects, which arise from differences in transition-state zero-point energies. In this case the effect arises from changes in the curvature of the mass-weighted PES, which in turn lead to different dynamics trajectories between the H- and D-substituted cases. The value of 1.4 is related to the $\sqrt{2}$ ratio of stretching frequencies of the CH and CD bonds broken in the reaction. Luch and co-workers located the VRI at a C–O bond length of 1.90 for O₂ addition to (deuterated) tetramethylethylene.^[45]

The ene reaction of allene **29** forms the C²–C⁶ cyclization product **30** (Figure 5).^[46,47] Singleton and co-workers have

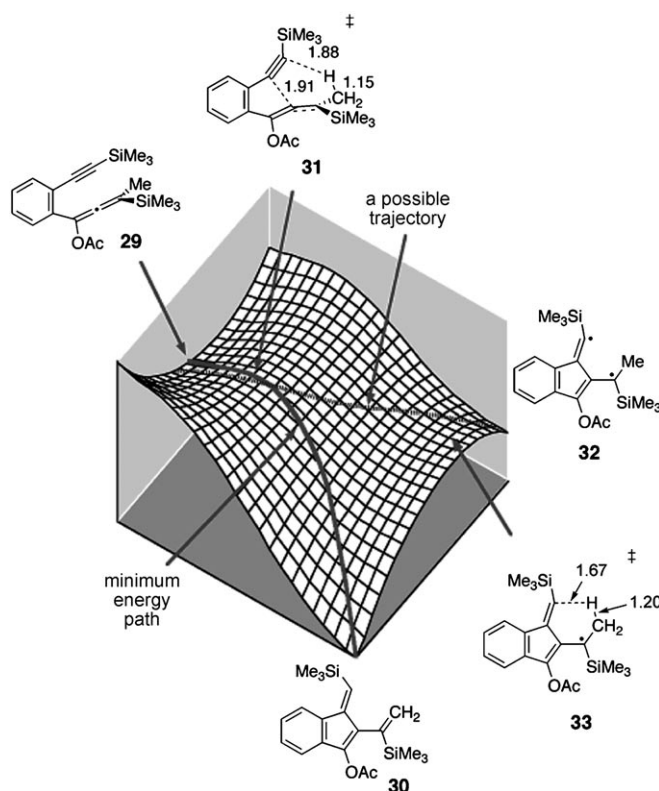


Figure 5. Qualitative unsymmetrical bifurcating PES for C²–C⁶ cyclization of allene **29** (UB3LYP/6-31G** TS geometries). Adapted with permission from reference [47]. Copyright 2005 American Chemical Society.

shown that there is a single “concerted” TS (**31**) that leads to either the ene product (**30**) or the diradical intermediate **32**. Figure 5 shows Singleton’s qualitative unsymmetrical bifurcating surface and B3LYP stationary points. Because the sequential transition states are offset, the MEP/IRC connects TS **31** to **30**. However, possible trajectories can pass over **31** and go to the diradical intermediate (**32**). The amount of **32** formed will depend on the exact shape of the surface. Quasiclassical dynamics simulations on a B3LYP surface showed that 29 out of 101 trajectories deviate from the MEP and form the diradical intermediate. This finding is consistent

with experimentally trapped diradical intermediates and the measured KIE (again, ca. 1.4), which is too large for a stepwise mechanism but too small for concerted. Schmitt et al. have recently confirmed this bifurcation model experimentally by observing large differences in intermolecular and intramolecular KIEs for several substituted versions of **29**.^[48]

4.4. Cycloadditions

Both Sakai and Nguyen^[49] and Cremer and co-workers^[50] have described the bifurcation on the PES for the concerted cycloaddition of *cis*-1,3-butadiene with ethylene. After the C_{2v} -symmetric Diels–Alder transition state, the reaction path bifurcates, leading to either of the possible half-chair cyclohexenes.

Caramella et al.^[51–54] brought the role of bifurcations to the attention of many chemists through the remarkable finding that some of the simplest Diels–Alder reactions involve surface bifurcations. In a series of papers, Caramella and co-workers have shown that endo dimerizations of methacrolein,^[51] cyclopentadiene,^[52] butadiene,^[53] and cyclopentadienone,^[54] occur along bifurcating reaction pathways. Previously, diene dimerization reaction selectivity was viewed as the result of competing transition states. Figure 6a shows a

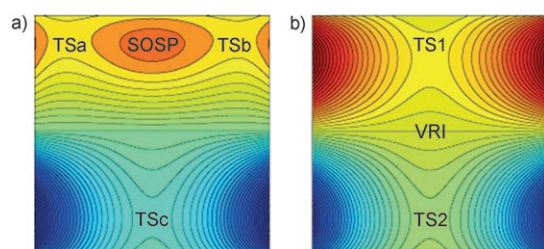
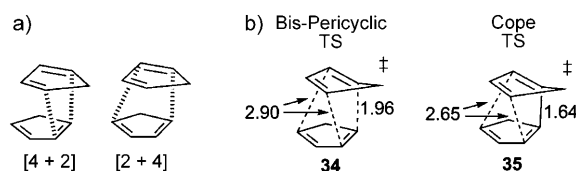


Figure 6. Model potential energy surface contour plots for a) pericyclic and b) bis-pericyclic cycloaddition. (high energy: red, low energy: blue).

model contour plot of a PES with two competing cycloaddition transition states, TSa and TSb, a second-order saddle point (SOSP) that connects them, and the Cope TS (TSd), corresponding to isomerization of the cycloadducts. In the diene dimerizations studied by Caramella and others,^[55] TSa and TSb have merged into a single “bis-pericyclic” transition state, TS1 (Figure 6b). On such a surface, the second-order saddle point is lost and a VRI point intervenes between the bis-pericyclic TS and the Cope transition state, TS2.

While there are two possible [4+2] cycloaddition pathways for cyclopentadiene dimerization (Scheme 7a), a single highly asynchronous Diels–Alder transition state, (**34**, Scheme 7b) is found. The primary [2+4] interactions are equal in magnitude to the [4+2] interactions, resulting in one short partial bond (1.96 Å) that is common to both interactions and two equivalent long partial bonds (2.90 Å). The IRC leads directly from **34** to the Cope transition state (**35**),



Scheme 7. Endo cyclopentadiene dimerization a) [4+2] interactions; b) transition-state structures from reference [52].

with only a slight decrease in energy (2.3 kcal mol^{−1}) and shortening of all three bonds. The two endo cycloaddition pathways have merged at the bis-pericyclic transition state and split at a VRI point between **34** and **35**, leading to one of two equivalent endo cycloadducts. Lasorne et al. located the valley–ridge inflection structure with partial bond lengths of 1.87 and 2.87 Å.^[56]

Houk and co-workers have studied a series of tethered (intramolecular) cyclobutadiene–butadiene cycloaddition reactions with bifurcating PESs.^[57] Figure 7 shows the influence

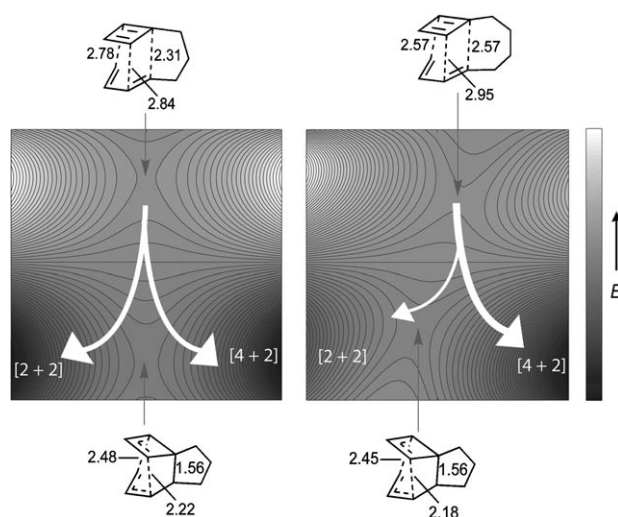
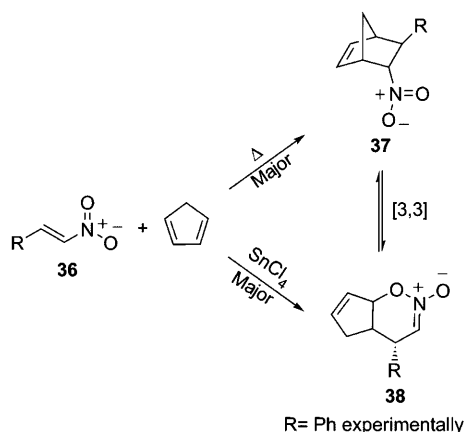


Figure 7. Qualitative PESs for cycloaddition of cyclobutadiene and butadiene with trimethylene and tetramethylene tethers. Energies and geometries taken from reference [57].

of the tether length on the transition-state structure and PES shape and branching ratios (white arrows) for trimethylene and tetramethylene tethers. The Diels–Alder and Cope transition states are nearly aligned relative to each other along the reaction coordinate in the trimethylene tether case and are predicted to give roughly equal ratios of [2+2] and [4+2] cycloadducts. The longer tetramethylene tether substantially offsets the positions of these transition states, resulting in a highly unsymmetrical surface with a large preference for formation of the [4+2] cycloadduct.

More recently, our group has found that periselectivity for cycloadditions of cyclopentadiene with nitroalkenes and α -keto- β,γ -unsaturated phosphonates under thermal and Lewis acid catalyzed conditions are controlled by a bis-pericyclic transition state.^[58] Under thermal conditions, cyclopentadiene acts as the 4π -diene component in the cycloaddition with

nitroalkenes **36**, and the Diels–Alder (DA) adduct **37** is the major product (Scheme 8). Selectivity is reversed with Lewis acid SnCl_4 , and the hetero-Diels–Alder (HDA) adduct (**38**) is



Scheme 8. Competing Diels–Alder and hetero-Diels–Alder cycloadditions of cyclopentadiene and nitroalkenes.

preferred. Figure 8 shows a qualitative comparison of the thermal and Lewis acid catalyzed bifurcating PESs with geometries of the bis-pericyclic Diels–Alder transition states (TS1) above and the Claisen rearrangement transition states (TS2) below each surface. Preference for the Diels–Alder adduct under thermal conditions is due to the shorter C–C bond compared to the C–O interaction. SnCl_4 coordination decreases the C–O bond length and increases the C–C distance, leading to a preference for C–O bond formation along the IRC. Effectively, SnCl_4 skews the bis-pericyclic transition state toward the hetero-Diels–Alder adduct, and

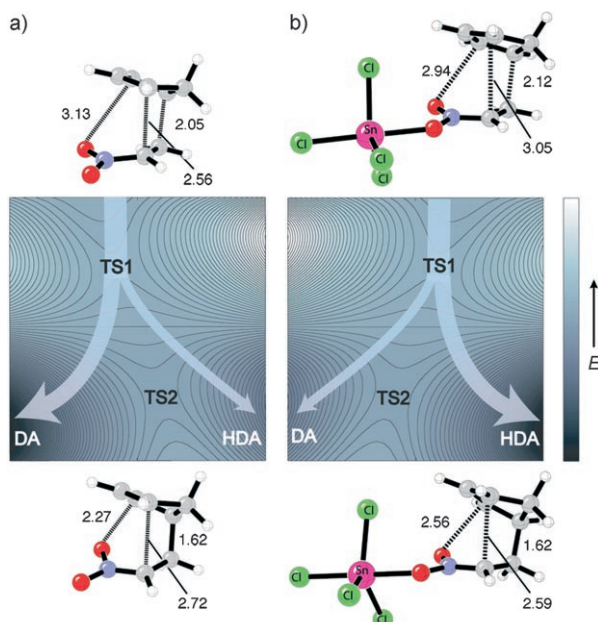


Figure 8. Qualitative contour plots and transition-state structures for a) thermal and b) Lewis acid catalyzed Diels–Alder cycloaddition of cyclopentadiene with nitroethene. Adapted with permission from reference [58]. Copyright 2007 American Chemical Society.

now only trajectories deviating significantly from the MEP lead to the Diels–Alder adduct.

Singleton and co-workers have also shown that the PES for the cycloaddition of cyclopentadiene with diphenylketene is unsymmetrical and that a common transition state leads to both $[4+2]$ and $[2+2]$ cycloadducts.^[59] Again, the rate-limiting transition-state geometry provides a good predictor of periselectivity, but there is no simple way to quantitatively predict branching ratios with dynamics simulations.

Bis-pericyclic transition states are also involved in complex cycloaddition reactions used in natural-product synthesis. For example, Quideau and co-workers have shown that a bis-pericyclic Diels–Alder transition state controls diastereofacial selectivity in the dimerization of *ortho*-quinols for the synthesis of (+)-aquaticol, a bis-sesquiterpene.^[60] Cycloaddition bifurcations were also reported for the reaction of 1,2,4,5-tetrazines and pyridazines with alkynes, the cycloaddition of cycloheptatriene and cyclopentadiene,^[61] 1,3-dipolar cycloadditions,^[62] and dichlorocarbene addition to cyclopropene.^[63]

5. Conclusions and Outlook

The possibility that multiple intermediates and/or products can be formed from a single transition state expands the scope of possible reaction pathways and complicates classic distinctions between stepwise and concerted mechanisms. Lluich and co-workers have proposed the use of variational transition state theory to predict product distributions in the case of symmetric bifurcating reaction pathways made unsymmetric by isotopic substitution.^[45] However, in general, when a PES bifurcation occurs, analysis of the entire potential energy surface is critical for a qualitative understanding of reaction pathways. Presently, molecular dynamics simulations are often necessary to give quantitative predictions of selectivity and isotope effects for these cases, since product distributions are no longer dictated by relative free energies of competing transition states.^[59]

The last decade has witnessed a flurry of reports of reaction pathway bifurcations in organic reactions, precipitated in part by the pioneering work of Caramella and co-workers on bis-pericyclic reactions.^[51–54] Future work will undoubtedly uncover many more examples of post-transition-state reaction pathway bifurcations in pericyclic reactions. The sundry examples described in this Minireview demonstrate that reaction pathway bifurcations are not mere curiosities, but may be quite general for many types of organic and organometallic transformations.^[64]

We are grateful to the National Science Foundation for financial support (CHE-0548209) and a traineeship to D.H.E. [NSF IGERT: Materials Creation Training Program (DGE-0114443)]. S.E.W. is supported by a NIH NRSA postdoctoral fellowship (NIH-1F32GM082114-01), while N.Ç.-Ö. is supported by the Scientific and Technological Research Council of Turkey (TÜBİTAK).

Received: February 25, 2008

Published online: September 2, 2008

- [1] B. K. Carpenter in *Reactive Intermediates Chemistry* (Eds.: R. A. Moss, M. S. Platz, M. Jones, Jr.), Wiley-Interscience, New York, **2004**.
- [2] P. Valtazanos, K. Ruedenberg, *Theor. Chim. Acta* **1986**, 69, 281.
- [3] D. A. Singleton, C. Hang, M. J. Szymanski, M. P. Meyer, A. G. Leach, K. T. Kuwata, J. S. Chen, A. Greer, C. S. Foote, K. N. Houk, *J. Am. Chem. Soc.* **2003**, 125, 1319.
- [4] M. Hamaguchi, M. Nakaishi, T. Nagai, T. Nakamura, M. Abe, *J. Am. Chem. Soc.* **2007**, 129, 12981.
- [5] a) See reference [21]; b) R. M. Minyaev, D. J. Wales, *Chem. Phys. Lett.* **1994**, 218, 413.
- [6] T. Fueno, *The Transition State*, Gordon and Breach, Tokyo, **1999**.
- [7] E. Kraka in *Encyclopedia of Computational Chemistry*, Vol. 4 (Ed.: P. von R. Schleyer), Wiley, New York, **1998**, p. 2445.
- [8] D. J. Wales, *J. Chem. Phys.* **2000**, 113, 3926.
- [9] K. Fukui, *Acc. Chem. Res.* **1981**, 14, 363.
- [10] B. K. Carpenter, *Acc. Chem. Res.* **1992**, 25, 520; C. Doubleday, M. Nendel, K. N. Houk, D. Thweatt, M. Page, *J. Am. Chem. Soc.* **1999**, 121, 4720.
- [11] W. Quapp, *J. Mol. Struct.* **2004**, 695–696, 95.
- [12] T. Taketsugu, N. Tajima, K. Hirao, *J. Chem. Phys.* **1996**, 105, 1933.
- [13] W. H. Miller, N. C. Handy, J. E. Adams, *J. Chem. Phys.* **1980**, 72, 99; J. González, X. Gliménez, J. M. Bofill, *J. Chem. Phys.* **2002**, 116, 8713.
- [14] W. Quapp, M. Hirsch, O. Imig, D. Heidrich, *J. Comput. Chem.* **1998**, 19, 1087; W. Quapp, M. Hirsch, D. Heidrich, *Theor. Chem. Acc.* **1998**, 1000, 285.
- [15] W. Quapp, M. Hirsch, D. Heidrich, *Theor. Chem. Acc.* **2000**, 105, 145; W. Quapp, M. Hirsch, D. Heidrich, *Theor. Chem. Acc.* **2004**, 112, 40; W. Quapp, *J. Theor. Comput. Chem.* **2003**, 2, 385.
- [16] A. Jiménez, R. Crehuet, *Theor. Chem. Acc.* **2007**, 118, 769.
- [17] I. H. Williams, G. M. MAggiora, *J. Mol. Struct.* **1982**, 89, 365.
- [18] Y. Kumeda, T. Taketsugu, *J. Chem. Phys.* **2000**, 113, 477.
- [19] B. Lasorne, G. Dive, M. Desouter-Lecomte, *J. Chem. Phys.* **2003**, 118, 5831.
- [20] S. M. Colwell, *Mol. Phys.* **1984**, 51, 1217; S. M. Colwell, N. C. Handy, *J. Chem. Phys.* **1985**, 82, 1281; J. Baker, P. M. W. Gill, *J. Comput. Chem.* **1988**, 9, 465; T. Yanai, T. Taketsugu, K. Hirao, *J. Chem. Phys.* **1997**, 107, 1137.
- [21] D. A. Hrovat, W. T. Borden, *J. Am. Chem. Soc.* **1992**, 114, 5879.
- [22] P. G. Wenthold, D. A. Hrovat, W. T. Borden, W. C. Lineberger, *Science* **1996**, 272, 1456.
- [23] O. Castaño, R. Palmeiro, L. M. Frutos, J. Luisandrés, *J. Comput. Chem.* **2002**, 23, 732.
- [24] O. Castaño, L.-M. Frutos, R. Palmeiro, R. Notario, J.-L. Andrés, R. Gomperts, L. Blancafort, M. A. Robb, *Angew. Chem.* **2000**, 112, 2168; *Angew. Chem. Int. Ed.* **2000**, 39, 2095.
- [25] W. A. Shapley, G. B. Bacskay, *J. Phys. Chem. A* **1999**, 103, 6624.
- [26] J. J. Finnerty, C. Wentrup, *J. Org. Chem.* **2004**, 69, 1909; J. J. Finnerty, C. Wentrup, *J. Org. Chem.* **2005**, 70, 9735.
- [27] N. Yamamoto, F. Bernardi, A. Bottoni, M. Olivucci, M. A. Robb, S. Wilsey, *J. Am. Chem. Soc.* **1994**, 116, 2064; S. Malone, A. F. Hegarty, M. T. Nguyen, *J. Chem. Soc. Perkin Trans. 2* **1988**, 477; I. V. Tokmakov, G.-S. Kim, V. V. Kislov, A. M. Mebel, M. C. Lin, *J. Phys. Chem. A* **2005**, 109, 6114.
- [28] S. Shaik, D. Danovich, G. N. Sastry, P. Y. Ayala, H. B. Schlegel, *J. Am. Chem. Soc.* **1997**, 119, 9237; G. N. Sastry, S. Shaik, *J. Am. Chem. Soc.* **1998**, 120, 2131.
- [29] J. Li, X. Li, S. Shaik, H. B. Schlegel, *J. Phys. Chem. A* **2004**, 108, 8526; V. Bakken, D. Danovich, S. Shaik, H. B. Schlegel, *J. Am. Chem. Soc.* **2001**, 123, 130.
- [30] H. Yamataka, M. Aida, M. Dupuis, *Chem. Phys. Lett.* **1999**, 300, 583; H. Yamataka, M. Aida, M. Dupuis, *Chem. Phys. Lett.* **2002**, 353, 310.
- [31] P. Valtazanos, S. T. Elbert, S. Xantheas, K. Ruedenberg, *Theor. Chim. Acta* **1991**, 78, 287; S. Xantheas, S. T. Elbert, K. Ruedenberg, *Theor. Chim. Acta* **1991**, 78, 327; S. Xantheas, S. T. Elbert, K. Ruedenberg, *Theor. Chim. Acta* **1991**, 78, 365; P. Valtazanos, K. Ruedenberg, *Theor. Chim. Acta* **1991**, 78, 397; P. Valtazanos, S. T. Elbert, K. Ruedenberg, *J. Am. Chem. Soc.* **1986**, 108, 3147; W. A. Kraus, A. E. DePristo, *Theor. Chim. Acta* **1986**, 69, 309.
- [32] D. H. Nouri, D. J. Tantillo, *J. Org. Chem.* **2006**, 71, 3686.
- [33] R. A. Bartsch, Y. M. Chae, S. Ham, D. M. Birney, *J. Am. Chem. Soc.* **2001**, 123, 7479.
- [34] D. A. Hrovat, J. A. Duncan, W. T. Borden, *J. Am. Chem. Soc.* **1999**, 121, 169.
- [35] W. R. Roth, D. Wollweber, R. Offerhas, V. Rekowski, H. W. Lennartz, R. Sustmann, W. Müller, *Chem. Ber.* **1993**, 126, 2701.
- [36] S. L. Debbert, B. K. Carpenter, D. A. Hrovat, W. T. Borden, *J. Am. Chem. Soc.* **2002**, 124, 7896.
- [37] C. P. Suhrada, C. Selçuki, M. Nendel, C. Cannizzaro, K. N. Houk, P.-J. Rissing, D. Baumann, D. Hasselmann, *Angew. Chem.* **2005**, 117, 3614; *Angew. Chem. Int. Ed.* **2005**, 44, 3548.
- [38] M. B. Reyes, E. B. Lobkovsky, B. K. Carpenter, *J. Am. Chem. Soc.* **2002**, 124, 641.
- [39] I. Özkan, M. Zora, *J. Org. Chem.* **2003**, 68, 9635.
- [40] L. M. Stephenson, M. J. Grdina, M. Orfanopoulos, *Acc. Chem. Res.* **1980**, 13, 419.
- [41] K. Yamaguchi, S. Yabushita, T. Fueno, K. N. Houk, *J. Am. Chem. Soc.* **1981**, 103, 5043; G. Tonachini, H. B. Schlegel, F. Bernardi, M. A. Robb, *J. Am. Chem. Soc.* **1990**, 112, 483.
- [42] M. Orfanopoulos, L. M. Stephenson, *J. Am. Chem. Soc.* **1980**, 102, 1417; M. B. Grdina, M. Orfanopoulos, L. M. Stephenson, *J. Am. Chem. Soc.* **1979**, 101, 3111.
- [43] A. G. Leach, K. N. Houk, *Chem. Commun.* **2002**, 2002, 1243.
- [44] D. A. Singleton, C. Hang, M. J. Szymanski, E. E. Greenwald, *J. Am. Chem. Soc.* **2003**, 125, 1176.
- [45] À. González-Lafont, M. Moreno, J. M. Lluch, *J. Am. Chem. Soc.* **2004**, 126, 13089.
- [46] P. G. Wenthold, M. A. Lipton, *J. Am. Chem. Soc.* **2000**, 122, 9265.
- [47] T. Bekele, C. F. Christian, M. A. Lipton, D. A. Singleton, *J. Am. Chem. Soc.* **2005**, 127, 9216.
- [48] M. Schmittel, C. Vavilala, R. Jaquet, *Angew. Chem.* **2007**, 119, 7036; *Angew. Chem. Int. Ed.* **2007**, 46, 6911.
- [49] S. Sakai, M. T. Nguyen, *J. Phys. Chem. A* **2000**, 104, 9169.
- [50] E. Kraka, A. Wu, D. Cremer, *J. Phys. Chem. A* **2003**, 107, 9008.
- [51] L. Toma, S. Romano, P. Quadrelli, P. Caramella, *Tetrahedron Lett.* **2001**, 42, 5077.
- [52] P. Caramella, P. Quadrelli, L. Toma, *J. Am. Chem. Soc.* **2002**, 124, 1130.
- [53] P. Quadrelli, S. Romano, L. Toma, P. Caramella, *Tetrahedron Lett.* **2002**, 43, 8785.
- [54] P. Quadrelli, S. Romano, L. Toma, P. Caramella, *J. Org. Chem.* **2003**, 68, 6035.
- [55] T. C. Dinadayalane, G. N. Sastry, *Organometallics* **2003**, 22, 5526; T. C. Dinadayalane, G. Gayatri, G. N. Sastry, J. Leszczynski, *J. Phys. Chem. A* **2005**, 109, 9310.
- [56] B. Lasorne, G. Dive, M. Desouter-Lecomte, *J. Chem. Phys.* **2005**, 122, 184304.
- [57] J. Limanto, K. S. Khuong, K. N. Houk, M. L. Snapper, *J. Am. Chem. Soc.* **2003**, 125, 16310.
- [58] N. Çelebi-Ölçüm, D. H. Ess, V. Aviyente, K. N. Houk, *J. Am. Chem. Soc.* **2007**, 129, 4528.
- [59] B. R. Ussing, C. Hang, D. A. Singleton, *J. Am. Chem. Soc.* **2006**, 128, 7594.
- [60] J. Gagnepain, F. Castet, S. Quideau, *Angew. Chem.* **2007**, 119, 1555; *Angew. Chem. Int. Ed.* **2007**, 46, 1533; J. Gagnepain, R. Méreau, D. Dejugnac, J.-M. Léger, F. Castet, D. Deffieux, L. Pouységu, S. Quideau, *Tetrahedron* **2007**, 63, 6493.
- [61] A. G. Leach, E. Goldstein, K. N. Houk, *J. Am. Chem. Soc.* **2003**, 125, 8330.

- [62] R. C. Mawhinney, H. M. Muchall, G. H. Peslherbe, *Can. J. Chem.* **2005**, 83, 1615.
- [63] D. C. Merrer, P. R. Rablen, *J. Org. Chem.* **2005**, 70, 1630; M. Khrapunovich, E. Zelenova, L. Seu, A. N. Sabo, A. Flaherty, D. C. Merrer, *J. Org. Chem.* **2007**, 72, 7574.
- [64] C. Zhou, D. M. Birney, *Org. Lett.* **2002**, 4, 3279; H. F. Bettinger, R. I. Kaiser, *J. Phys. Chem. A* **2004**, 108, 4576; L. Chen, H. Xiao, J. Xiao, X. Gong, *J. Phys. Chem. A* **2003**, 107, 11440.

Feeling the Chemistry...

Better Looking, Better Living, Better Loving

How Chemistry can Help You Achieve Life's Goals

John Emsley *Ampthill, Bedfords., Great Britain*

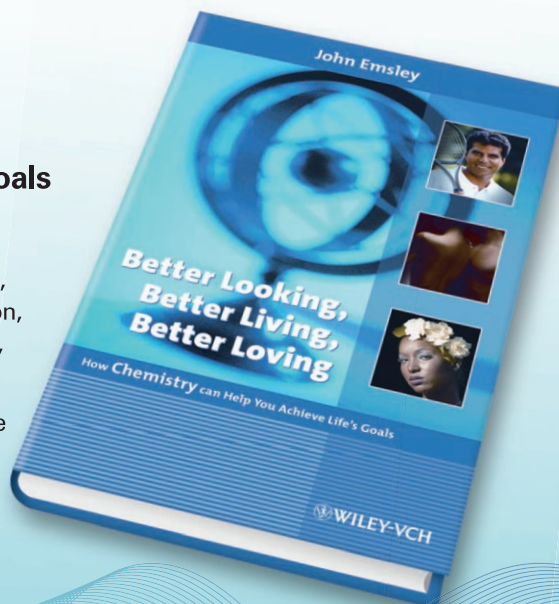
Welcome to a tour of some of the recent advances in chemistry, taking in the cosmetic factory, the pharmacy, the grooming salon, the diet clinic, the power plant, the domestic cleaning company, and the art gallery along the way.

Award-winning popular science writer John Emsley is our guide as he addresses questions of grooming, health, food, and sex. The trip is for all those of us wanting to know more about the impact of chemical products on our everyday lives.

May 2007

ISBN: 978-3-527-31863-6

249 Pages • Hardback



 **WILEY-VCH**

13059